

CHARACTERIZATION OF FATIGUE DAMAGE IN LONG FIBER EPOXY COMPOSITE LAMINATES

Simone Giancane*, Francesco W. Panella*, Vito Dattoma*

*** Department of Ingegneria dell'Innovazione, Università del Salento, Italy
via per Arnesano, 73100 Lecce, Italy**

Keywords: *fatigue, damage, long fiber, epoxy*

Abstract

A study and characterization of a GFRC material is here presented. Forty fatigue tests (twenty for each of the two considered stacking sequence) have been carried out and by means of them S-N curves have been traced. Two quantities have been chosen for monitoring damage evolution during each test: stiffness and dissipated energy per cycle. The presence of three zones in obtained graphs can be observed and it is evident that the most important and dangerous structural transformations take place only in very final part of life. This consideration seems to be confirmed by the analysis of micrographies effected on fractured specimens and also on only partially damaged specimens.

1 Introduction

The first case in which composite materials have been widely employed in modern structures is the Apollo 14 mission in earlier seventies. In that occasion aluminium and fiber reinforced material were used [1]. In last two decades all advanced industrial fields (aeronautical, cars racing, ...) make use of composite materials for highly stressed components during life and their employment will increase, because new industrial processes allow to obtain even more performing materials.

In this work, long fiber laminates are considered, because they cover a broad spectrum of composite parts and, in particular, fatigue damage of GFRC is studied.

Fatigue phenomena for a GFRC laminate are very complex to be analyzed because of the presence of numerous interfaces that cause a continuous stress redistribution into the representative volume element and in the whole component too. Anyway three

important processes of damage evolution have been identified: fiber crack formation in on-axis plies, matrix crack formation in off-axis plies and in correspondence of fiber crack tips, growing delaminations among plies [2,3]. These phenomena are interacting among themselves and it is impossible to clearly distinguish their mutual onset and their termination; moreover the percentage of life in which one of them is predominant varies in dependence on fiber-matrix, stacking sequence and test conditions (presence of notches, load, temperature, ...) [4]. Numerous constitutive models describing fatigue behaviour of long fiber composite exist in literature and in some cases they are quite suitable to predict cycles to failure or variation of some variable related to damage with opportune margins, but none of them, for what briefly exposed, is able to take into account all or the most part of physical aspect of laminate damage [5-7].

This paper presents a study on fatigue effects for epoxy matrix composites with long E-glass fiber. A large number of specimens has been tested under traction in order to monitor the damage state at various stress state and to establish the effective correlation with experimental data.

Two important parameters are considered as evolving with damage: stiffness and absorbed mechanical energy. Both of them show common features not independently with the total test duration and this encourages interesting damage state valuations.

2 Materials and specimen geometry

The specimens have been manufactured in laboratory using unidirectional E-glass fibers (600 g/m²) and epoxy matrix with lay-up technique. The mechanical properties of components are reported in table 1 as follows.

Table 1. Mechanical properties of E-glass fibers and epoxy resin.

<i>E-glass fibers</i>	
Average value of Diameter (μm)	10
Young Modulus (MPa)	73000
Ultimate tensile strength (MPa)	3400
Strain to failure (%)	4.8
<i>Epoxy Resin EC 130 LV + Hardening Additive W340 (ratio 100:37) (ALTANA VARNISH-COMPOUNDS)</i>	
Density (g/ml)	1,14÷1,16
Young Modulus (MPa)	2900÷3100
Ultimate tensile strength (MPa)	75÷80
Strain to failure (%)	8,5÷9

In order to achieve reliable laminate performances, avoiding air inclusions into the resin and near the fiber-matrix interfaces, a special additive (L9505 - BYK) has been used; every laminate has been produced in the same humidity and temperature condition (25 °C and 20 % of relative humidity). After placement each ply in its orientation, the epoxy resin has been accurately deposited and manually conditioned for perfect adhesion with the fiber plies and the laminate has been pressed at 1.7 bar for 24 hours in controlled atmosphere. A mean volume percentage of fibers of 40 % has been obtained and the composite has been finally cured at a temperature of 60 °C for 15 hours.

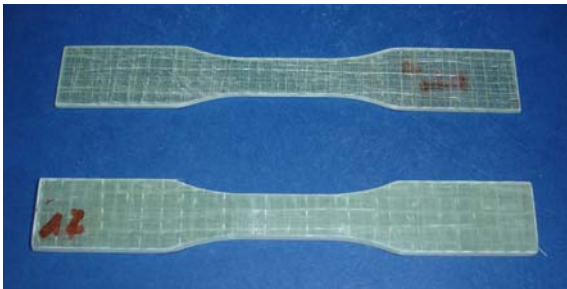


Fig. 1. Two specimens with different stacking sequence and identical geometry.

The specimen geometry in figure 2 has been adopted; using specimens with large fillet radius of 60 mm is possible to reduce stress concentrations and at the same time to use simple hydraulic grips without additional tabs.

Taking as reference the longitudinal specimen axis, two different stacking sequences have been considered: $[0/90/0/90]_s$ and $[90/0/0/90]_s$.

From every 300 mm \times 300 mm plate, 20 specimens have been obtained, for a total of 60 specimens. The laminate thickness is 4.3 mm.

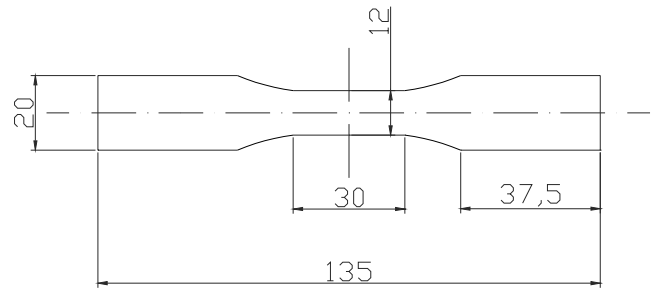


Fig. 2: Geometry of the flat specimen.

3 Test details and data processing

The specimens have been extracted from three plates obtained in the same work and environment conditions and marked with the letters A, F and G. From each slab, a total of 20 specimens have been obtained and numbered: first 10 in the $[0/90/0/90]_s$ configuration and second 10 for $[90/0/90/0]_s$ lay-up. Two specimens, randomly chosen for each slab and with different stacking sequence, have been statically tested and the results are reported in figure 3. The crossbar speed crossbar has been set at 0.5 mm/min. They show good reproducibility and coherence as can be seen in table 1.

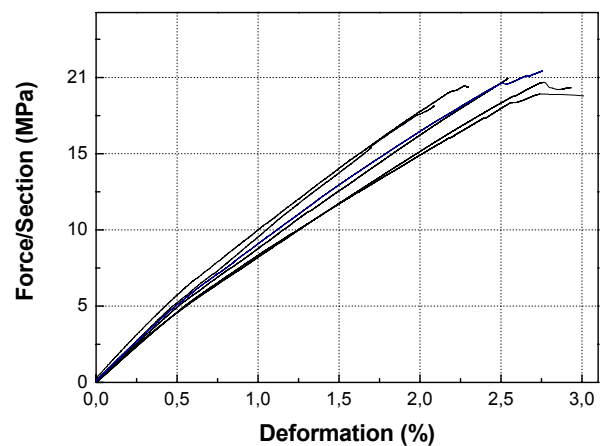


Fig. 3. Static tests for six specimens that are reported in table 1.

Sinusoidal fatigue load has been applied with a frequency of 15 Hz and a load ratio R equal to 0.1. Two variables have been considered as significant index of damaged state of material: stiffness variation and dissipated energy per cycle into the specimen during fatigue test. The stiffness (E) has been calculated cycle by cycle averaging the value derived from ascending and descending sides of the load cycle. Deformation of a specimen under cyclic

load is a process that dissipates energy during the increasing load phase; a part of this energy is released back during the load decreasing and a residual part is consumed to create new defects or propagate the existing ones [8-10]. Therefore the hysteresis area per cycle during fatigue tests represents a not-direct index of general damage state: higher is the absorbed strain energy, more important is the damage process which takes place. Dissipated energy is henceforth indicated with symbols H and by means of a opportune algorithm (figure 4) it has been possible to consider each complete closed cycle and calculate it cycle by cycle. The other parameter considered as damage index is residual stiffness [11].

Table 2. General scheme for static tests.

Specimen ID	Lay-up	Rupture Force (N)	Rupture deformation (%)	Ultimate strenght (MPa)	E (MPa)
A4	(0/90/0/90) _s	19383	3.04	375.6	18240
A18	(90/0/90/0) _s	18679	2.08	362.0	20200
F10	(0/90/0/90) _s	19520	2.29	378.3	21300
F15	(90/0/90/0) _s	20590	2.54	399.0	19300
G1	(0/90/0/90) _s	19939	2.93	386.4	17840
G12	(90/0/90/0) _s	21081	2.75	408.5	19600

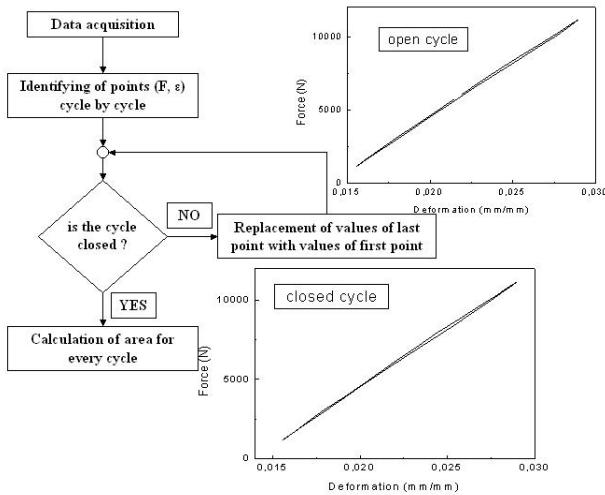


Fig. 4. Pseudo-code for calculation of H at each cycle.

Data acquisition has been performed storing 5 cycles every 50 and with a time step of $2.2 \mu s$ (corresponding to 450 Hz) from a life range from 2000 to 1500000 cycles. All tests have been conducted on a MTS multi purpose machine with a load cell of 100 kN and table 2 summarizes the test data specifications.

Test ID	Cycles to failure	Applied Load (Force/Section) _{at}	Test ID	Cycles to failure	Applied Load (Force/Section) _{at}
A9	2714	121 MPa	A15	1886	121 MPa
A5	12812	121 MPa	G13	3600	121 MPa
A8	2489	105 MPa	F12	4092	105 MPa
F5	3321	105 MPa	F14	5324	105 MPa
A6	17737	105 MPa	F19	5072	105 MPa
F7	5186	105 MPa	A13	18343	105 MPa
A3	25667	105 MPa	A14	41190	105 MPa
G7	10638	105 MPa	G15	8592	105 MPa
A9	6080	91 MPa	A12	494200	91 MPa
A7	83720	91 MPa	A11	520391	91 MPa
A1	98080	91 MPa	F16	12557	91 MPa
F3	5360	91 MPa	F13	18873	91 MPa
F8	4817	91 MPa	A17	417144	91 MPa
G8	15594	91 Mpa	F17	84135	91 Mpa
A10	491050	83 MPa	A20	542975	83 MPa
A2	102880	83 MPa	A19	1437820	83 MPa
F4	29920	83 MPa	A16	1209620	83 MPa
F2	20272	83 MPa	F20	20292	83 MPa
F6	19365	83 MPa	F11	31299	83 MPa
F9	12593	83 MPa	F18	127010	83 MPa

Adopting the “constant stress level method”, the fatigue life curves have been determined considering three load levels and, fitting this results according to Weibull statistical analysis [12] (fig 5 and 6). On graphs are also reported the experimental data not taken into account for statistical analysis and marked in curly brackets.

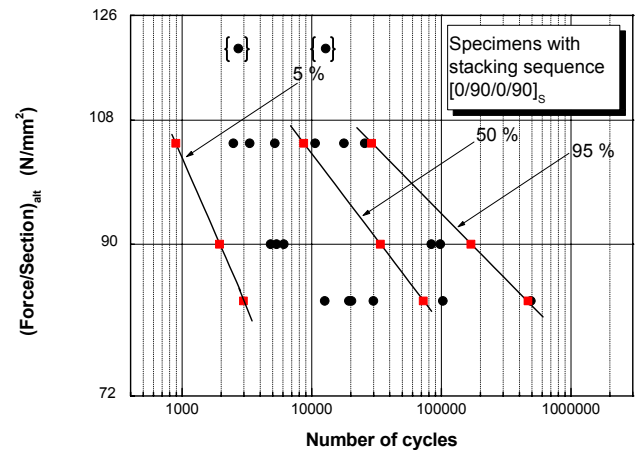


Fig. 5. S-N Curves for fatigue tests conducted on $[0/90/0/90]_s$ specimens. The points defining the probability curves of rupture are marked with red squares.

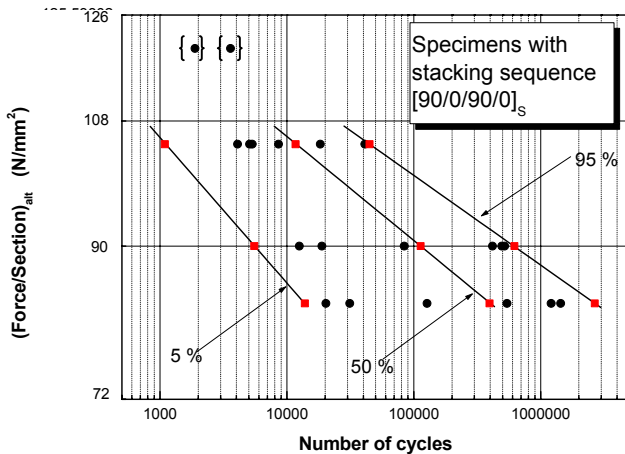


Fig. 6. S-N Curves for fatigue tests conducted on $[90/0/90/0]_s$ specimens. The points defining the probability curves of rupture are marked with red squares.

4 Experimental Results

Both E and H have been calculated as referred to specimen central zone for a length of 10 mm (indicated with the peak “loc”), instrumented with an extensometer of same gage length and, at the same time, to total portion of material between the grips (indicated with “tot”).

For each test, all the measures are reported on diagrams as function of N with normalized scale on x and y axis with respect to maximum calculated values for E , H and $N_{failure}$. This procedure allows to better compare different test measures with various load levels.

Comparing E^{tot} and H^{tot} with E^{loc} and H^{loc} , it is possible to also identify the damaged zone in the central monitored zone or outside it. Considering specimen A7 as example, the measures of dissipated energy as calculated for the central part and for the entire specimen have the same trend and similar values, indicating that damage mainly interests the central zone (figures 7a and 7b). This interpretation is confirmed by the trend of E^{tot} and E^{loc} : the two diagrams show very good agreement and it means that stiffness reduction mainly takes place in the portion of material with the extensometer.

For other tested specimens, different behaviour has been observed and the damage mainly evolves also in the immediacy of filleted zone. Taking as significant example the specimen F17, it can be observed that E^{loc} and H^{loc} maintain constant values for the whole test duration while “tot” measures point out a clear decrease of E and a large increase of dissipated energy evidencing the continue and progressive evolution of fatigue damage.

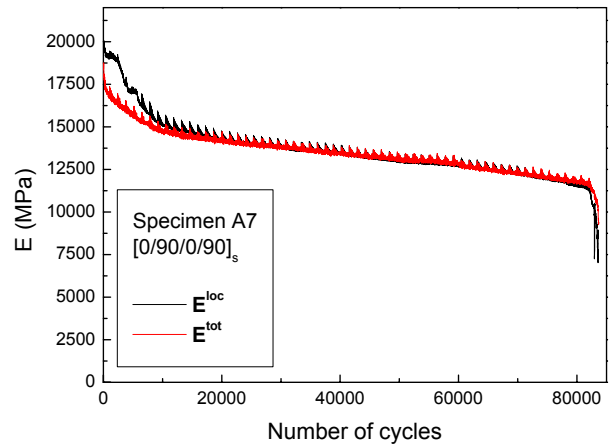


Fig. 7a. Measures of E elaborated for specimen A7 that presents rupture in its central zone.

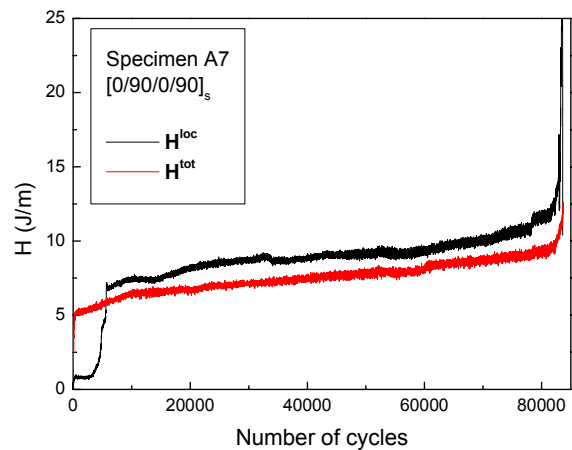


Fig. 7b. Measures of H elaborated for specimen A7 that presents rupture in its central zone.

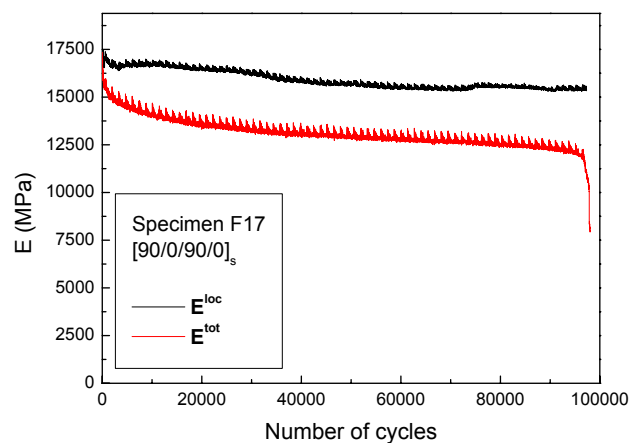


Fig. 8a. Measures of E elaborated for specimen F17 that presents rupture in its filleted zone.

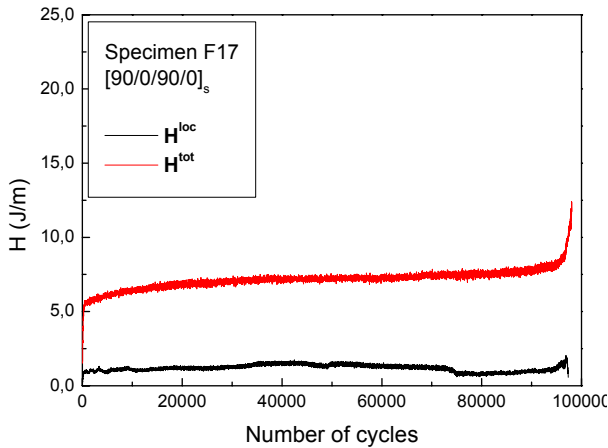


Fig. 8b. Measures of H elaborated for specimen F17 that presents rupture in its filleted zone.

Considering E^{tot} and H^{tot} normalized curves for all tests (figure 9a and 9b), two slope transition points can be observed at curves extremities; they exist in correspondence of a certain consumed life percentage level and therefore is possible to identify three zones corresponding to main stiffness and dissipated energy behavior. The following considerations can be easily highlighted from figures 9 a-b:

1. the slope transition points for H^{tot} and E^{tot} values in each test show good correspondence in term of consumed life; they are generally positioned around 5% and 95% of total time.
2. the damage curves can be approximated with three linear segments (one for each zone) as displayed for instance in figure 10 for test A20;
3. the coefficients a_2 b_2 c_2 and d_2 , defining the stabilized central part of the damage curves can be analysed for different specimens; they are found to be nearly constant and independent from the load level and from the stacking sequence as displayed in figures 11, 12, 13 and 14, in which low dispersion for H^{tot} and especially for E^{tot} coefficients is observed.

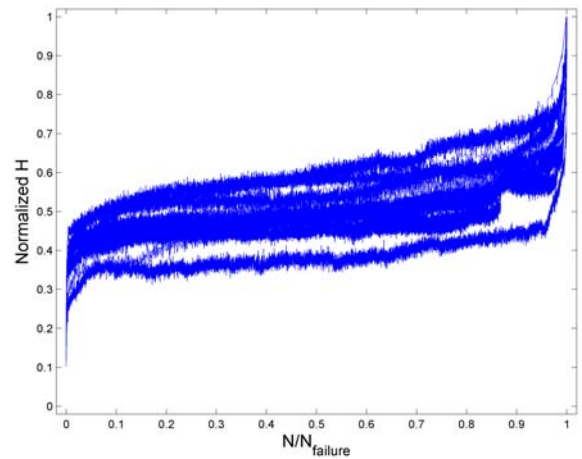


Fig. 9a. All measures for and H^{tot} reported as superposed and in normalized coordinates.

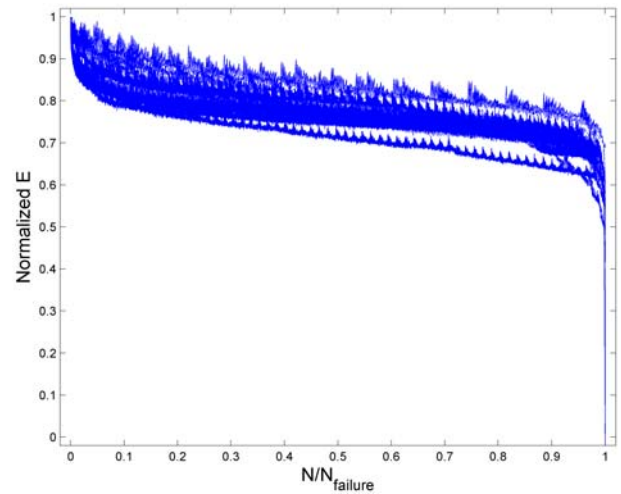


Fig. 9b. All measures for E^{tot} reported as superposed and in normalized coordinates.

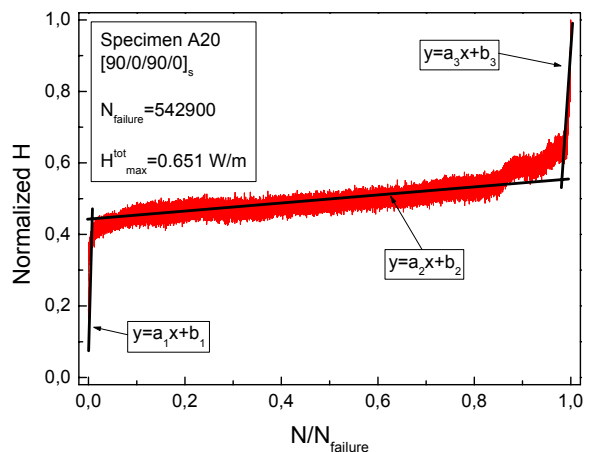


Fig. 10a. Linear approximation of normalized H curve for specimen A20.

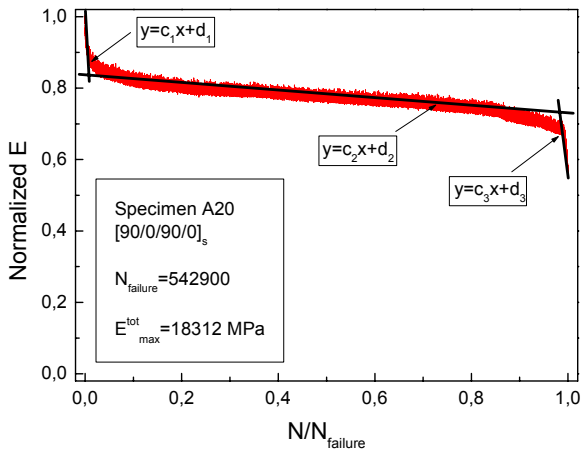


Fig. 10b. Linear approximation of normalized E curve for specimen A20.

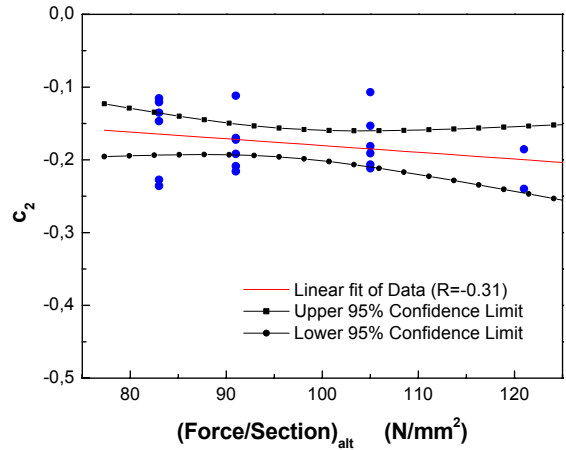


Fig. 13. Parameter c_2 calculated for all conducted fatigue test (rif.: fig 10b).

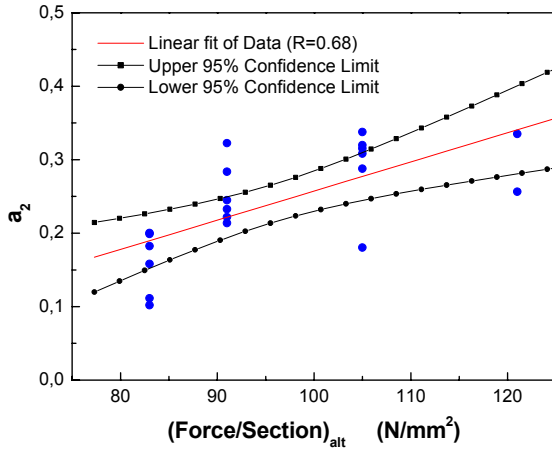


Fig. 11. Parameter a_2 calculated for all conducted fatigue test (rif.: fig 10a).

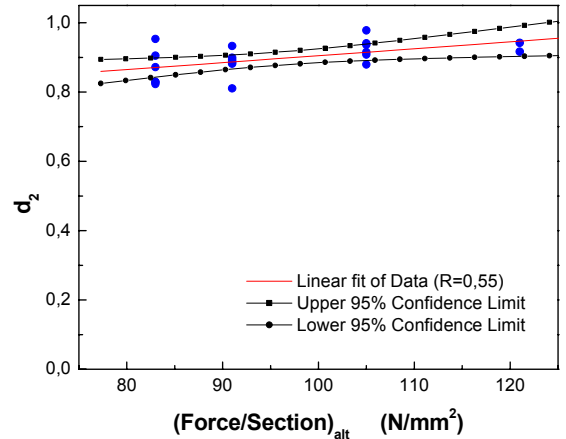


Fig. 14. Parameter d_2 calculated for all conducted fatigue test (rif.: fig 10b).

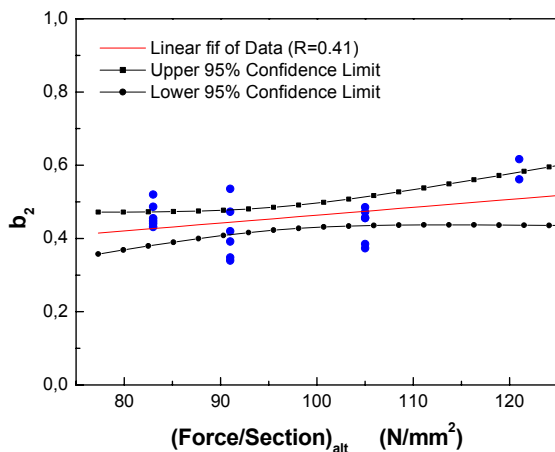


Fig. 12. Parameter b_2 calculated for all conducted fatigue test (rif.: fig 10a).

Concerning with figures 9a and b, the initial phase is dominated by elevated stiffness E assessment with a sensible and fast decrease in the order of 15÷20 %, until a stable value is reached; this fact points out that the performances of composites strongly depends on time and initial fluctuating load values and this is presumably induced by internal matrix-fiber interactions with localized micro-slippage phenomena among plies until equilibrium of forces is reached. According to this, a visible energy dissipation increment is generated before a stable damage evolution process takes place.

The third and final damage phase is the classic rupture behaviour before failure, characterized by coalescence of defects and elevated stiffness drop induced by fiber breaks and matrix tearing with local plies separation. On the other hand, the stable phase is the most interesting, primarily because it occupies the largest part of

consumed life and is clearly placed in the same percentual life interval for all the specimens (figures 9a and 9b) either for E data trend, either for dissipated energy variations H . In addition, the monitored data seem to converge to constant values in this phase and the damage behaviour can be considered as linear with constant slope for each load level; the knowledge of the extrapolated damage data however may be useful to estimate the damage state in the component in terms of residual life to failure, provided that constant load amplitude is applied and consistent stiffness and energy measures are performed.

Diagrams in figures 11 and 13 resume the slope data trend a_2 and c_2 (fig. 11-a, 11,c) and the coefficients b_2 and d_2 calculated for H measures and stiffness E variations in the stable phase versus applied load. Though data are referred to specimens with $[0/90/0/90]_s$ and $[90/0/90/0]_s$ stacking sequences and differently loaded, b_2 , c_2 and d_2 coefficients seem to settle at a constant level ($b_2 = 0.45$ and $d_2 = 0.9$) within 95% confidence limits, while a_2 seems to have a light increase for higher load. Other tests with intermediate level with respect the considered ones could lightly modify the obtained results but anyway the most important result which emerges from the experimental data and their computation is a common evolution of all specimens damage state that results independent from load condition (in the considered range), lay-up sequence and number of cycles to failure.

5 Analysis of micrographies

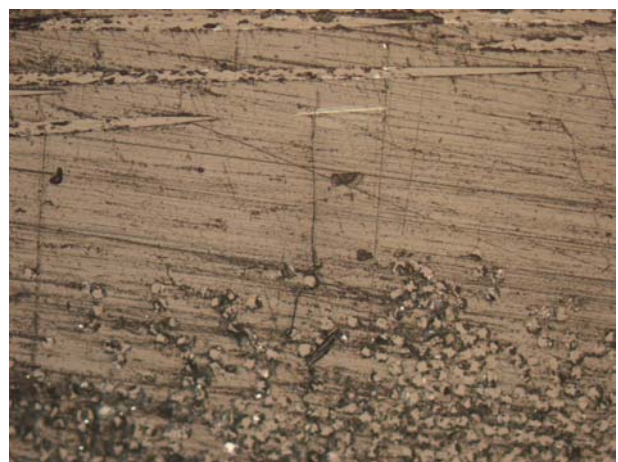
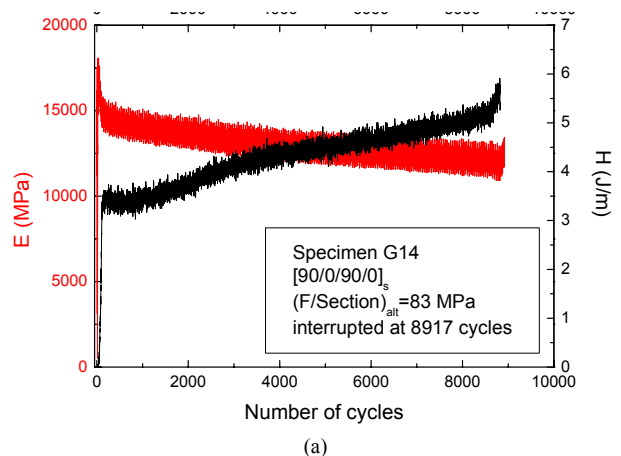
The presence of three distinguishable zones in graphs of E^{tot} and H^{tot} is associated with the evolution of damage mechanics that follow three main steps [molta bibliografia]:

- Matrix cracks formation in the off axis plies forming a pattern called CDS
- Fiber cracks due to the redistribution of stress near the primary matrix crack tips
- Delamination in zones in correspondence of primary matrix crack tips

The last two events here exposed take place only in final part of life for the studied material, showing relevant energy absorption increment and a abrupt stiffness drop; they can be considered as contemporaneous and bring quickly material to definitive fracture. On the contrary, matrix cracks are present since the very first cycles and continue to evolve in a stable phase, being largely responsible of damage evolution during central part of fatigue life of specimen.

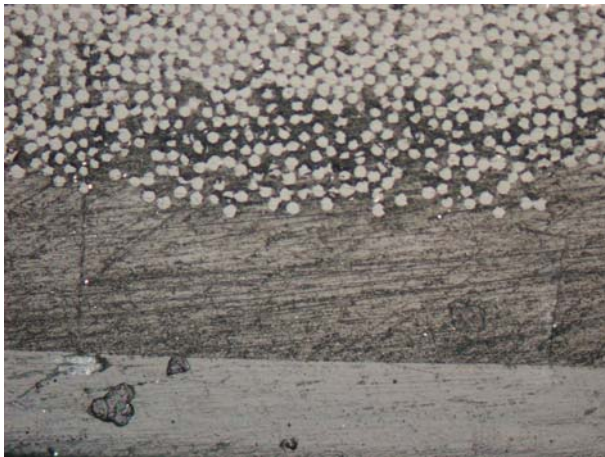
A possible confirmation of this concept is given by the analysis of micrographies for partially damaged specimens. Some tests have been carried out and interrupted in correspondence of the central zone. In figure 15, small cracks can be observed for specimen G14. They seem to have origin from micro-defects (microvoids or impurities) or from fiber in off-axis plies but do not initiate from the interface of adiacent plies; no crack progapagate beyond a single layer and they are stopped by the fibers of on-axis plies.

A different situation is observable for specimen A11 (see table 2) for which a section in proximity of rupture surface has been investigated. Micrographies show important cracks that cross the section of specimen in all its layers. Moreover a wide delamination among plies is also visible. These observations show that the most important events that bring GFRC to fatigue failure take place only in the last part of life and that they become catastrophic in few cycles.





(c)

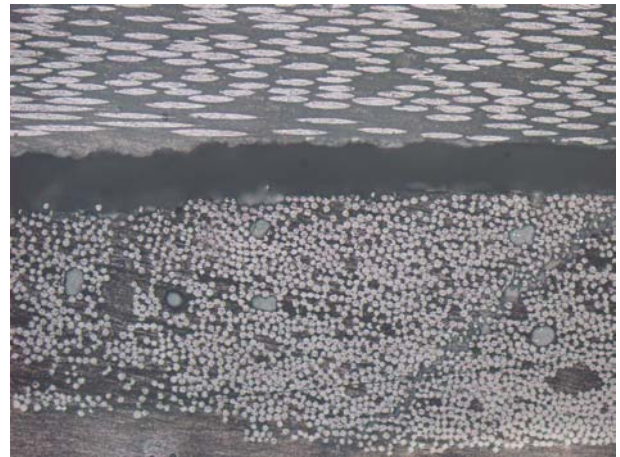


(d)

Fig. 15. (a) E^{tot} and H^{tot} of G14 test interrupted at 8917 executed cycles; (b,c,d) micrographies of the surface obtained by a longitudinal cleavage of specimen G17.



(a)



(b)

Fig. 16. Two micrographies of the surface obtained by a trasversal cleavage near fillet of specimen A11. In the (a) figure the presence of important crack can be observed; in (b) figure a wide delamination among plies has been caught.

6 Conclusions

A study of fatigue damage of a GFRC has been presented. At first, static characterization has been conducted and then forty fatigue rupture tests have been performed (twenty specimens for each stacking sequence). S-N curves have been sketched and, for the same tests, two quantities has been chosen as damage index: stiffness (E) and dissipated energy per cycle (H). Analyzing the considered measures, the presence of three well-defined zones has been observed for all tests, no matter for the load condition or for stacking sequence. So, fatigue damage evolution seems to have an important progress in the very first part and especially in the last part of life. This aspect is confirmed by the analysis of micrographies; in fact, some partially damaged specimen show small cracks that interest only one layer at times and no delamination can be relieved; on the contrary, micrographies of a section of a fractured specimen show that before final rupture important damage phenomena interest the material and long cracks and wide delamination among plies are present.

References

- [1] *Project: Apollo 14*. Release NO:71-3K, NASA 1971.
- [2] Reifsnider K. L. *Damage and Damage Mechanics, Fatigue of Composite Materials, Cap. 2*, pp 11-77, Edited by K.L. Reifsnider, 1990.
- [3] Talreja R.. Multi-scale modelling in damage mechanics of composite materials. *Journal of Material Science*, Vol. 41, pp 6800-6812.

- [4] O' Brein T.K. Damage in composite Materials: Basic Mechanism Accumulation, Tolerance, and Characterization. *ASTM STP 775*, Edited by K.L. Reifsnider, 1982.
- [5] Degrieck J., Van Paepegem W. Fatigue Damage Modelling of Fibre-reinforced Composite Materials: Review, *Applied Mechanics Reviews*, Vol. 54(4), 279-300, 2001.
- [6] Ladevèze P. A damage computational method for composite structures. *Comput Struct*, Vol. 44(1/2), pp 79-87, 1992.
- [7] Shokrieh M.M, Lessard L.B. Multiaxial fatigue behavior unidirectional plies based on uniaxial fatigue experiments – I Modelling. *International Journal of Fatigue*, Vol. 19, No. 3, pp 201-207, 1997.
- [8] Peyroux R., Chrysochoos A., Licht C., Lobel M. Thermomechanical coupling and pseudelasticity of shape memory alloys, *International journal of science*, pp. 489-509, 1998.
- [9] Dharan C.K.H., Tan T.F. A hysteresis-based damage parameter for notched composite laminates subjected to cycle loading, *J Mater Sci*, Vol. 42, pp 2204-2207.
- [10] Iannucci L., Ankersen J. An energy based damage model for thin laminated composites, *Composite Science and Technology*, Vol. 66, pp. 934-951, 2006.
- [11] Kuo W.-S., Pon B.-J. Elastic moduli and damage evolution of three-axis woven fabric composites, *Journal of Material Science*, Vol. 32, pp. 5445-5455, 1997.
- [12] Little R.E., Jebe E.H. *Statistical design of fatigue experiments*, applied science publishers LTD, 1975.